Developmental Cell, Vol. 8, 611–622, April, 2005, Copyright ©2005 by Elsevier Inc. DOI 10.1016/j.devcel.2005.01.015

The Stomach Mesenchymal Transcription Factor Barx1 Specifies Gastric Epithelial Identity through Inhibition of Transient Wnt Signaling

Byeong-Moo Kim,[1,2] Georg Buchner,[3] Isabelle Miletich,[3] Paul T. Sharpe,[3] and Ramesh A. Shivdasani[1,2,*]
[1]Department of Medical Oncology and Department of Cancer Biology
Dana-Farber Cancer Institute
[2]Department of Medicine
Brigham & Women's Hospital and Harvard Medical School
Boston, Massachusetts 02115
[3]Institute for Craniofacial Biology
Kings College
London SE1 9RT
United Kingdom

Summary

Inductive interactions between gut endoderm and the underlying mesenchyme pattern the developing digestive tract into regions with specific morphology and functions. The molecular mechanisms behind these interactions are largely unknown. Expression of the conserved homeobox gene *Barx1* is restricted to the stomach mesenchyme during gut organogenesis. Using recombinant tissue cultures, we show that Barx1 loss in the mesenchyme prevents stomach epithelial differentiation of overlying endoderm and induces intestine-specific genes instead. Additionally, Barx1 null mouse embryos show visceral homeosis, with intestinal gene expression within a highly disorganized gastric epithelium. Barx1 directs mesenchymal cell expression of two secreted Wnt antagonists, sFRP1 and sFRP2, and these factors are sufficient replacements for Barx1 function. Canonical Wnt signaling is prominent in the prospective gastric endoderm prior to epithelial differentiation, and its inhibition by Barx1-dependent signaling permits development of stomach-specific epithelium. These results define a transcriptional and signaling pathway of inductive cell interactions in vertebrate organogenesis.

Introduction

Developmental patterning along the cephalocaudal axis of the vertebrate gastrointestinal (GI) tract distinguishes the caudally positioned intestine from a rostral organ that serves mechanical and chemical functions in digestion. Animals have evolved a diverse array of specialized structures to this end, including the avian gizzard and proventriculus and the mammalian stomach. Little is known about how distinctive GI epithelia are specified.

By embryonic day (E) 9 in the mouse, the primitive gut tube is marked rostrally by a radially enlarged gastric anlage and caudally by the elongated intestine, although endodermal cell morphology remains uniformly undifferentiated until about E12. Subsequent patterning leads to differentiation of characteristic epithelia within each organ. The adult intestinal mucosa projects innumerable villi, lined by limited cell types (Cheng and Leblond, 1974; Stappenbeck et al., 1998), whereas the stomach epithelium houses 11 distinct cell lineages that organize within deep pits and contiguous glands (Karam et al., 1997). In response to chronic tissue injury in adult life, humans frequently convert gastric epithelium into an intestinal type. Such intestinal metaplasia, the precursor to nearly all cancers of the gastroesophageal junction and a high proportion of gastric corpus tumors (Reid et al., 2000), represents stereotypic reversal of normal development (Silberg et al., 2002; Slack, 1985).

Tissue grafting experiments reveal the source of mesenchyme to be an important determinant of gut endoderm differentiation (Kedinger et al., 1986; Mizuno and Yasugi, 1990), a theme that recurs in development of diverse organs like teeth and lungs (Tucker and Sharpe, 2004; Warburton et al., 2000). Small bowel endoderm from 6-day-old chick embryos develops proventricular (glandular stomach) architecture when cocultured with 6-day-old proventricular mesenchyme but fails to mature fully, as reflected in the lack of *pepsinogen* gene expression (Hayashi et al., 1988). In contrast, stomach endoderm from 14-day-old rat embryos develops features of the stomach epithelium when grafted in contact with intestinal mesenchyme (Duluc et al., 1994). These studies evaluated tissues starting at developmental stages when epithelial character may already be specified; while they are informative regarding requirements for cytodifferentiation, they are not necessarily so for lineage determination. In contrast, the unspecified E7 mouse endoderm receives instructive signals, including fibroblast growth factors, that determine its anteroposterior axis (Wells and Melton, 1999). Subsequently, selected foregut segments respond to signals secreted from adjacent heart or notochord cells that permit liver and pancreas differentiation, respectively (Hebrok et al., 1998; Jung et al., 1999; Rossi et al., 2001). These and other studies point to a window (approximately E8–E12 in the mouse) in which endoderm responds sequentially and regionally to specification signals.

The effects of well-characterized ligands, including bone morphogenetic (BMP), Wnt, and hedgehog (Hh) proteins, on gut epithelial cytodifferentiation have been investigated, for the most part, after the endoderm is committed to gastric or intestinal cell fate. Endoderm-derived Hh proteins influence both epithelial and muscle differentiation in the GI tract of chick (Roberts et al., 1995; Sukegawa et al., 2000), *Xenopus* (Zhang et al., 2000), and mouse (Ramalho-Santos et al., 2000; van den Brink et al., 2001) embryos, in part by inducing BMP-4 (Roberts et al., 1998; Sukegawa et al., 2000). Conversely, mesenchymal cells secrete Wnt proteins in complex patterns along the intestinal crypt-villus axis; Wnt ligands produced near the crypt base restrict differentiation of neighboring epithelial progenitors (van

*Correspondence: ramesh_shivdasani@dfci.harvard.edu

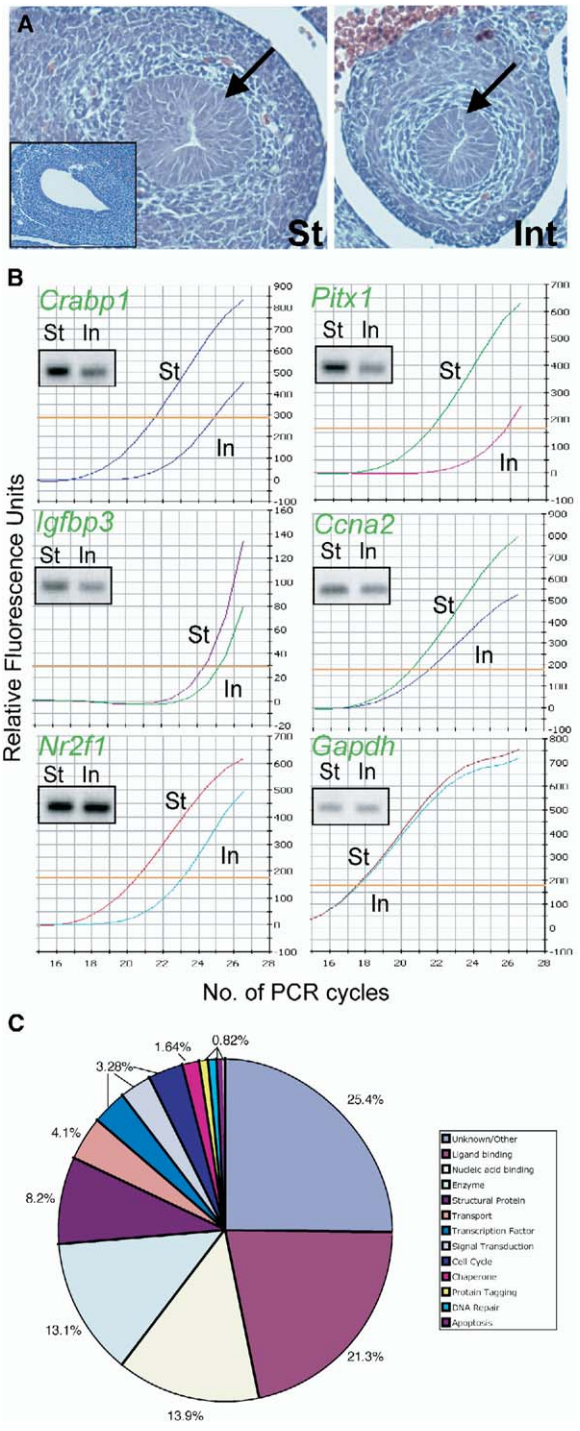

Figure 1. Differential Gene Expression in the E12 Mouse Stomach and Small Intestine

(A) Comparative histology of the target fetal tissues, revealing similar features; the rostral stomach (St, inset; It, intestine) is more differentiated. Arrows point to the endoderm.

(B) Validation of transcripts enriched in E12 stomach (St) by real-time RT-PCR. Curves in each panel trace the appearance of amplified DNA with increasing numbers of PCR cycles, and each inset shows ethidium bromide-stained PCR products after 28 cycles. Results are shown for five sample genes, *Crabp1*, *Igfbp3*, *Nr2f1*, *PitX1*, and *Ccna2*, and the *Gapdh* loading control.

(C) Pie chart representation of functional categories of 122 gene products that show significantly ($p < 0.015$) enriched expression in E12 St, grouped according to Gene Ontology designations.

de Wetering et al., 2002). The segmental expression of homeodomain proteins suggests that transcription factors (TFs) of this class may respond to local cues and convey vital positional information along the GI tract (Beck et al., 2000; Roberts et al., 1995; Yokouchi et al., 1995). Indeed, interference with normal mesenchymal Hox gene expression in vertebrate embryos causes diverse GI developmental anomalies (Aubin et al., 2002; Kondo et al., 1996; Pollock et al., 1992; Roberts et al., 1998; Warot et al., 1997; Wolgemuth et al., 1989). In contrast, inactivation of mouse *Pdx1* or *Cdx2* results in heterotopic conversion of epithelia in which these homeobox genes are normally expressed: pancreas and intestine, respectively (Chawengsaksophak et al., 1997; Jonsson et al., 1994). Other mesenchymal TFs, like Fkh6 and Foxl1, modulate postmitotic differentiation of subjacent stomach and intestinal epithelia in adults (Kaestner et al., 1997; Perreault et al., 2001). Taken together, these studies point to a combination of interaction-dependent and cell-autonomous facets of gut development, regulated in part by regionally restricted TFs.

Early in GI development, expression of the homeobox gene *Barx1* is confined to the stomach mesenchyme. Through epithelial-mesenchymal coculture and mutant mouse experiments, we establish a requirement for Barx1 in stomach development. Moreover, we find that Barx1 functions predominantly to regulate *sFRP1* and *sFRP2*, genes that reduce local Wnt activity. These signals act on endoderm to direct stomach epithelial differentiation and distinguish the target cells from an alternative intestinal fate.

Results

Comparison of Gene Expression in the E12 Mouse Stomach and Intestine

We used Serial Analysis of Gene Expression (SAGE; [Velculescu et al., 1995]) to compare gene profiles between the E12 fetal mouse stomach and intestine (Figure 1A). Because mRNAs associated with tissue maturity appear later (after E13 in the intestine; [Lepourcelet et al., 2005; Stappenbeck et al., 1998]), comparison at E12 might reflect the basis for tissue differentiation. The salient disparities are listed in Table S1 (see the Supplemental Data available with this article online), and the full data set is available in searchable form at http://genome.dfci.harvard.edu/StomSAGE. All tested differences were reproduced in independently derived tissue samples (Figures 1B, five examples shown). Among 122 differentially expressed transcripts ($p < 0.015$), 21% encode ligand binding proteins, equal fractions of 13% each encode nucleic acid binding proteins or enzymes, and 8% encode structural proteins (Figure 1C). Most profiling methods, including SAGE, tend to underestimate TF mRNAs, which are present at low concentrations. Our comparison in the fetal GI tract, however, highlighted differential expression of several TFs, in-

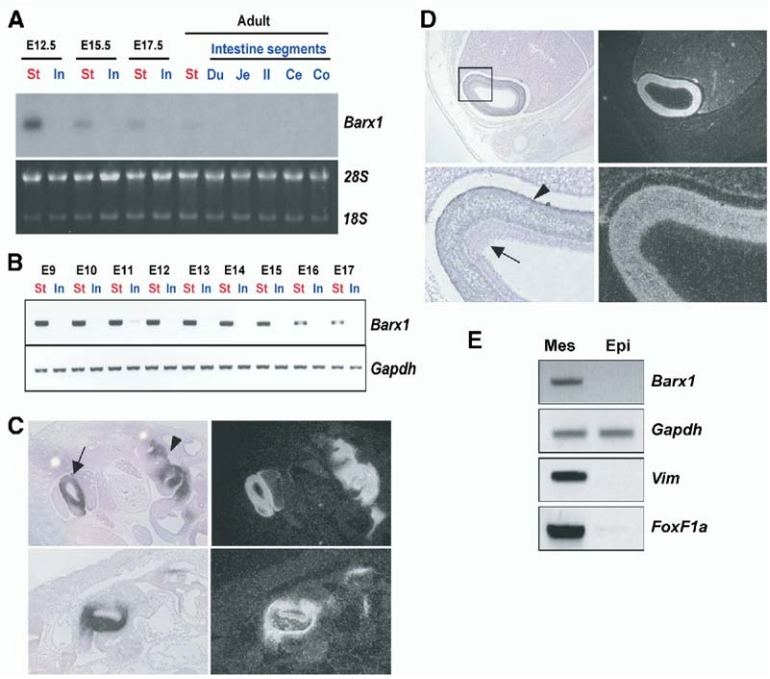

Figure 2. Barx1 Expression in Mouse Development

(A) Northern analysis of adult and fetal mouse stomach (St) and intestine (In) at the indicated stages. Du, duodenum; Je, jejunum; Il, ileum; Ce, cecum; Co, colon. Ethidium bromide staining of 28S and 18S rRNAs indicates equal sample loading.

(B) RT-PCR analysis of *Barx1* and *Gapdh* (loading control) in St and In over an extended developmental period.

(C) Radioactive Barx1 in situ hybridization at E11.5 (left, bright field; right, dark field) shows the stomach (arrow) and jaw (arrowhead) as the major sites of expression; rostral is to the right, and caudal is to the left. The lower panels (high magnification) highlight radially asymmetric Barx1 distribution in the stomach wall.

(D) Details of in situ hybridization in the E13.5 stomach reveal that Barx1 expression is confined to the mesenchymal compartment (arrowhead) and excluded from the endoderm (arrow). The two lower images represent the area boxed in the upper-left panel.

(E) The latter result is verified by RT-PCR on separated E12 stomach epithelial and mesenchymal cells; vimentin (Vim) and FoxF1a are known mesenchymal transcripts.

cluding homeodomain proteins Pitx1 and Barx1. Indeed, *Barx1*, a member of the subgroup defined by *Drosophila* BarH1, showed the highest dissimilarity of any transcript: 92 tags in the fetal stomach library and just 1 in the intestine ($p = 4e^{-20}$; total tags, ~65,000).

Barx1 expression was reported previously in the fetal mouse stomach (Tissier-Seta et al., 1995) and chick embryo proventriculus (Barlow et al., 1999; Smith et al., 2000). We confirmed and extended these findings. *Barx1* mRNA is absent from the developing and adult intestine, and its levels in the stomach peak at E13.5, with barely a trace detected in the neonatal or adult organ (Figures 2A and 2B). In situ hybridization localizes Barx1 to the jaw primordium and stomach mesenchyme (Figures 2C and 2D). We verified the latter result by RT-PCR analysis on tissue samples in which endodermal and mesenchymal cells were separated physically (Figure 2E); *Barx1* mRNA expression parallels that of two other mesenchymal markers, Vimentin and FoxF1. Levels of the closest homolog, *Barx2*, are much lower and do not vary appreciably along the GI tract (data not shown). In contrast, the highly restricted expression of Barx1 suggests a role in stomach development.

Mesenchymal Barx1 Controls Epithelial Differentiation in Overlying Endoderm

Homotypic or heterotypic fetal gut cultures in immunocompromised mice permit morphologic assessment of organ development but are not readily amenable to molecular manipulation of the grafted cells. This limitation can be overcome in large part if tissue primordia are cultured in physical contact ex vivo. Although the required degree of cellular disaggregation precludes evaluation of tissue morphology, molecular markers associated with cytodifferentiation can provide a reliable substitute.

To evaluate Barx1 functions, first we separated the E12.5 mouse stomach mesenchyme from its overlying stratified endoderm and established short-term cultures (Figure 3A). The cultured mesenchymal monolayer readily supported growth and differentiation of GI epithelia and could be transfected with DNA or small interfering (si) RNA molecules. Barx1 expression declined very slightly over the culture period (data not shown), which contrasts with its extinction in vivo and enabled our experimental design. The cells also induced robust expression of a complete panel of stomach epithelium-specific transcripts (Mucin-1, Gastrin, Intrinsic factor, and Lactoferrin) in gastric endoderm harvested from E12.5 mouse fetuses and cultured over the mesenchyme for 7 days (Figure 3C). Stomach epithelial differentiation was strictly organ specific, as cultured cells failed to express five intestinal markers (Figure 3D; intestinal and liver fatty acid binding proteins, Mucin-2, Defensin-2, and Cdx2). Likewise, intestine-derived cocultures followed intestinal differentiation faithfully, whereas crosscultures between stomach epithelium and intestinal mesenchyme, or vice versa, yielded inconsistent and weak expression of lineage-specific mRNAs (data not shown). In these and the following studies, we used sensitive RT-PCR for molecular markers to verify the absence of crosscontaminating cells, as illustrated in Figure 2E.

Treatment of the stomach mesenchyme with Barx1-specific siRNAs caused selective loss of *Barx1* mRNA and protein (Figure 3B). In contrast, Barx2-specific siRNAs reduced their cognate target but did not affect Barx1 levels and thus served as a negative control. siRNA-induced Barx1 deficiency had a dramatic and specific effect on the fate of overlying gastric endo-

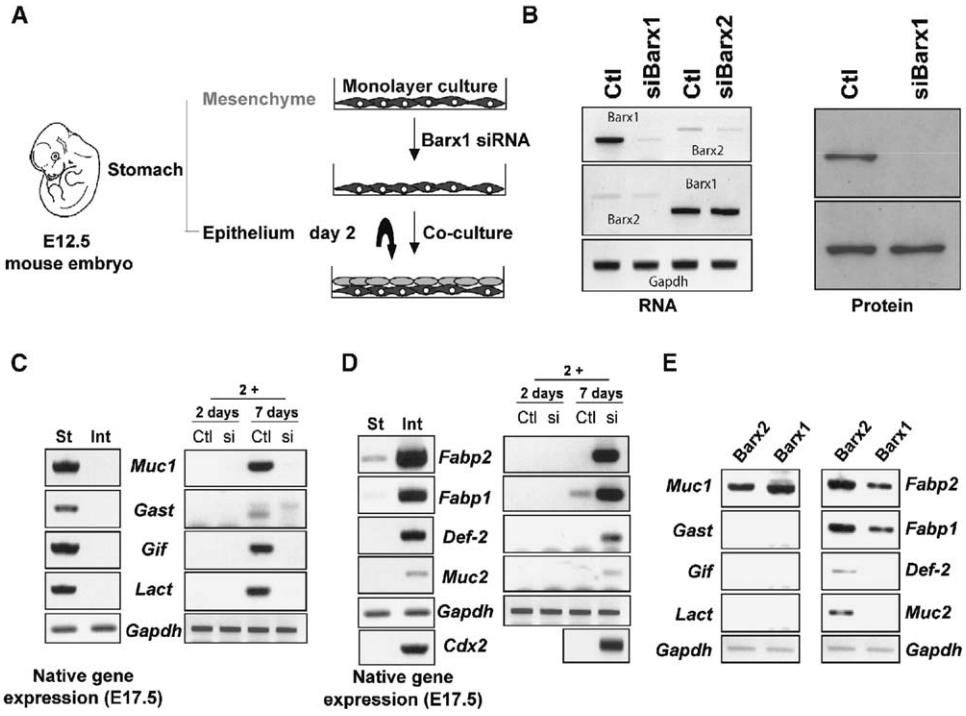

Figure 3. Barx1 Loss Reverses GI Epithelial Cell Type

(A) Experimental schema. E12 mouse stomach mesenchyme is isolated, cultured (endoderm is discarded), and treated with siRNA the next day. One day later, E12 mouse stomach endoderm is isolated separately and cultured over the mesenchymal monolayer for another 5–7 days.

(B) Evidence that treatment with Barx1-specific siRNAs reduces *Barx1* mRNA (left, RT-PCR) and protein (right, immunoblot) levels selectively and significantly.

(C and D) Organ-specific expression of (C) four stomach and (D) five intestinal epithelial transcripts at E17.5 (left panels). Right panels: E12 stomach endoderm cultured over mesenchyme treated without siRNA (data not shown) or with Barx2 siRNA (Ctl) selectively expresses stomach-specific genes, whereas coculture with Barx1 siRNA-treated mesenchyme causes loss of gastric epithelial markers and expression of intestine-specific transcripts. Results are representative of seven independent experiments.

(E) Forced expression of Barx1 in E12 intestinal mesenchyme attenuates intestine-specific transcripts in cocultured intestine-derived endoderm and increases expression of the gastric marker *Muc1*.

derm: all tested intestinal markers were activated (Figure 3D), and this occurred at the expense of all stomach-specific genes (Figure 3C). These findings are highly reproducible and implicate Barx1 as a key mesenchymal mediator of GI epithelial cell fate. In complementary experiments, forced expression of Barx1 (but not Barx2) cDNA in intestinal epithelial-mesenchymal cocultures consistently reduced expression of intestine-specific transcripts and enhanced expression of the stomach-specific gene *Muc1* (Figure 3E).

Defective Stomach Development in Barx1 Null Mice

Mouse Barx1 is encoded by four exons, and the homeodomain spans exons 2 and 3. We targeted this gene locus by homologous recombination in ES cells and generated mice in which parts of exons 2 and 4 and all of exon 3 are replaced by a neomycin-resistance cassette (Figure 4A). Homozygote embryos die around E13; reasons behind the lethality are under investigation and will be reported separately. We could nevertheless evaluate gut morphogenesis, which revealed a shrunken and malformed stomach but normal intestinal morphology, in E12.5 mutant embryos (Figure 4B). Most significantly, instead of starting to assume adult mucosal form, the Barx1$^{-/-}$ stomach lining is infolded, disorganized, and fails to open a lumen rostrally (panels 1" and 2" in Figure 4E). Although epithelial viability occasionally is compromised, as evidenced by the plug of dead cells shown in panel 3" (Figure 4E), the major abnormality is a failure to differentiate (Figures 4E and 4F), a defect that is especially marked in cephalic segments (cardia and corpus). In the antrum and pylorus, by contrast, the main finding is a heaping of undifferentiated epithelium in 5–6 cell layers, where tall columnar cells ordinarily are present in 2–3 cell layers (Figure 4G). Compared to normal littermates, which show concentric rings of fusiform mesenchyme, corresponding cells in the mutant, normally the site of Barx1 expression (Figure 2D), are also highly disarrayed (best seen in Figures 4F and 4E, panel 1"). Intestine development is unaffected (Figures 4B and 4D), and Barx1$^{-/-}$ embryos are grossly indistinguishable from their littermates at E12.5 (data not shown).

Although intestinal villus morphogenesis occurs after Barx1$^{-/-}$ embryos die, *Cdx2* expression, a specific marker of the intestine (Silberg et al., 2000), begins

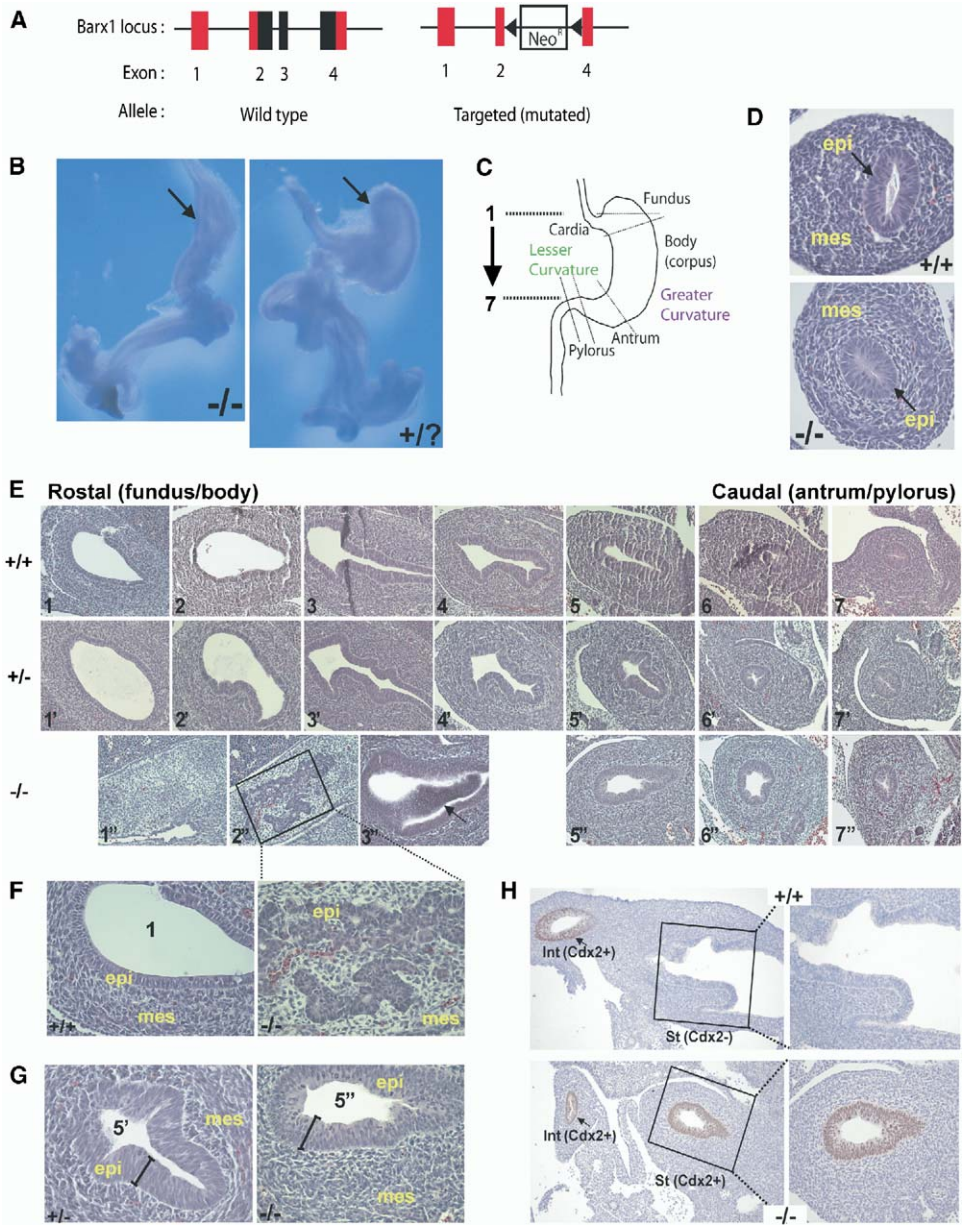

Figure 4. Defective Stomach Development in Barx1$^{-/-}$ Mice

(A) Gene targeting strategy, which replaced parts (black boxes) of *Barx1* exons 2–4 with a *LoxP*-flanked neomycin-resistance (Neo^{R}) cassette in reverse orientation and under control of the phosphoglycerate kinase promoter.

(B) Gross appearance of Barx1$^{-/-}$ (left) and littermate control (+/?, right) GI tracts, showing altered size and shape of the stomach (arrows), with sparing of the intestine.

(C) Diagram of defined regions in stomach anatomy, which correspond approximately to levels 1–7 of the tissue sections shown below.

(D) Histologic comparison of the small bowel from control (top) and Barx1$^{-/-}$ E13 embryos.

(E) Serial histology of Barx1$^{+/+}$, heterozygote (+/–), and nullizygous E13 fetal stomach, from rostral (left) to caudal regions. An arrow in panel 3″ points to a collection of nonviable cells.

(F–G) High-power images of selected tissue sections (panels 1, 2″, 5', and 5″ from [E]), which emphasize epithelial disorganization in the (F) body and piling of antral cells in (G) Barx1$^{-/-}$ stomach (right) compared to the corresponding levels in control samples (left).

(H) Immunostaining for the intestine marker Cdx2 (left, low magnification; right, high magnification) in the E12.5 GI tract in Barx1$^{-/-}$ embryos and control littermates. St, stomach; Int, intestine.

earlier. Cdx2 is predictably absent from the normal E12.5 stomach but is expressed ectopically in the defective epithelium of Barx1$^{-/-}$ stomach (Figure 4H); this is evident even in the prospective antrum, where the tissue morphology is affected minimally. Abnormal stomach morphology in the absence of Barx1 may thus

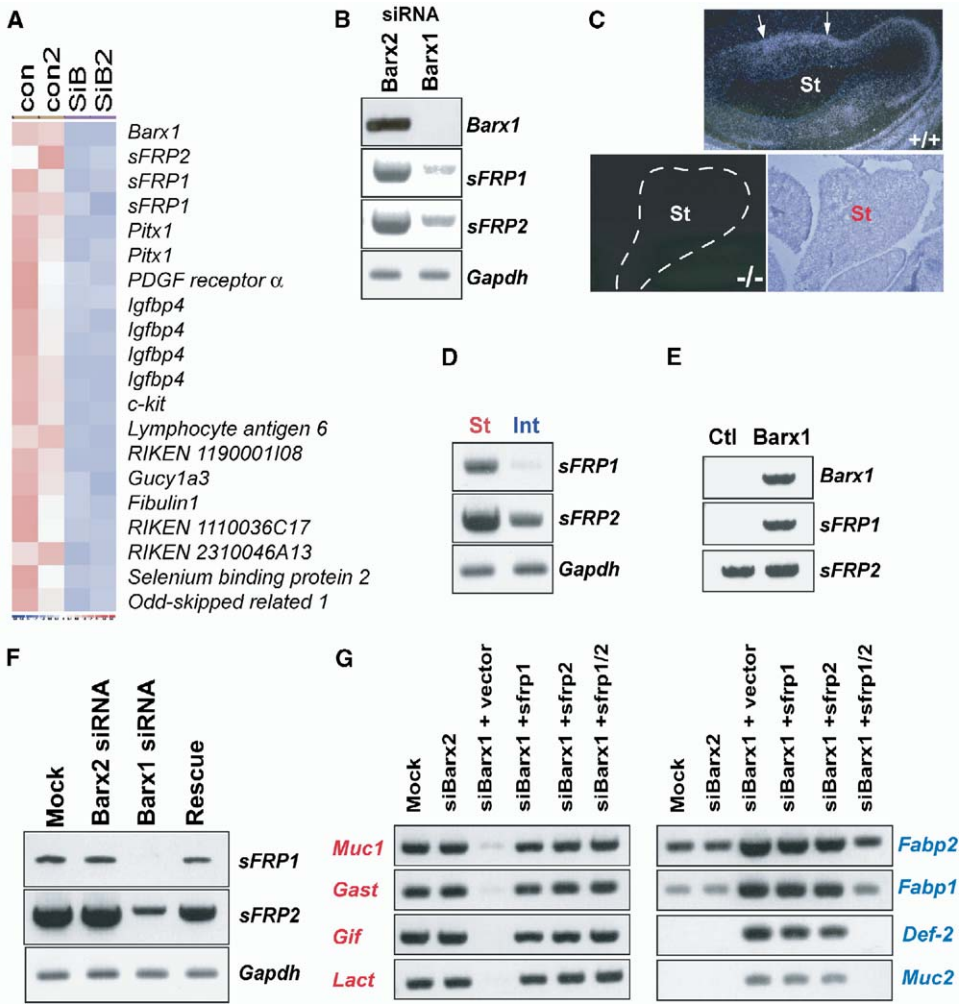

Figure 5. Rescue of Barx1 Loss by sFRPs

(A) Relative expression of transcripts significantly reduced in two independent experiments with cultured E12 mouse stomach mesenchyme treated with either control (Barx2; con) or Barx1-specific (siB) siRNAs. The left panels illustrate the original hybridization data for individual probe sets, with higher signals depicted in pink and lower signals depicted in blue.

(B) RT-PCR verification of reduced Barx1, sFRP1, and sFRP2 transcripts in independently treated cells.

(C) Radioactive in situ hybridization confirms loss of *sFRP2* mRNA in E13 Barx1$^{-/-}$ stomach (lower panels; dark- and bright-field images of the same microscope field) compared to wild-type. Signal development and photomicrograph exposures were identical; other sites of sFRP2 expression showed no difference.

(D) Native expression of *sFRP1* and *sFRP2* mRNAs in wild-type E13.5 stomach (St) and small intestine (Int), assessed by RT-PCR.

(E) RT-PCR demonstration of sFRP1 and sFRP2 expression induced in cultured intestine mesenchyme after transfection of Barx1 cDNA but not empty vector (Ctl).

(F) RT-PCR analysis confirms loss of sFRP transcripts after Barx1 siRNA treatment and recovery with transfection of the respective cDNAs.

(G) Expression of gastric epithelial markers, lost after Barx1-specific siRNA treatment of mesenchymal cells, is fully restored upon forced expression of sFRP1, sFRP2, or both cDNAs. A corresponding decrease in ectopically expressed intestine-specific markers is best observed with cotransfection of sFRP1 and sFRP2. The results represent four independent experiments.

reflect homeosis (posteriorization) in the rostral GI endoderm.

Loss of Barx1 Affects Levels of Secreted Wnt Antagonists

The presence of a homeobox motif in Barx1 suggests a transcriptional regulatory function, and our results imply that Barx1 controls genes that have paracrine activity. To identify such signals, we used oligonucleotide microarrays to decode the expression profiles of mesenchymal cells in which Barx1 is reduced by siRNA treatment. Compared to cells that received either Barx2-specific siRNAs or mock treatment (both these controls had nearly identical profiles), expression of only 14 transcripts was notably decreased, suggesting a limited role for Barx1 in gene regulation (Figure 5A). These transcripts included *Pitx1* and *Igfbp4*, genes that are considerably enriched in the developing stomach relative to intestine (Figure 1 and data not shown). Prominent among the downregulated products were

the secreted Frizzled-related proteins *sFRP1*, represented in two independent probe sets, and *sFRP2*. Both genes encode secreted polypeptides that prevent Wnt ligands from binding to surface receptors and hence modulate Wnt activity negatively (Finch et al., 1997; Rattner et al., 1997). We confirmed that Barx1 deficiency reduced cellular levels of *sFRP1* and *sFRP2* mRNAs (Figures 5B and 5C). Moreover, RT-PCR analysis of E13 mouse intestine and stomach demonstrated substantially enriched expression of these genes in the latter (Figure 5D). Recent studies independently reported strong sFRP expression early in development of the chicken gizzard, a stomach homolog; expression in the small intestine occurs later (McBride et al., 2003; Theodosiou and Tabin, 2003). Finally, forced Barx1 expression in cultured mouse intestinal mesenchyme induced *sFRP1* and *sFRP2* mRNAs (Figure 5E). The data thus strongly suggest that Barx1 regulates these transcripts positively in the developing stomach.

To determine the significance of this regulation, we attempted to rescue the epithelial specification defect associated with loss of mesenchymal Barx1 expression. After treatment of cultured stomach mesenchyme with Barx1-specific siRNAs, and prior to overlaying endoderm, we transfected the cells with expression constructs encoding sFRP1 and sFRP2; expression of the foreign genes was comparable to endogenous transcript levels (Figure 5F). Expression of sFRP1 and sFRP2, alone or in combination, reproducibly reversed differentiation of endoderm cultured over Barx1-deficient mesenchyme: expression of stomach epithelium-specific genes was restored fully, and intestinal markers were correspondingly attenuated, especially with the combination of sFRPs (Figure 5G). These factors are hence sufficient to overcome the absence of Barx1, whose control over endodermal cell fate appears to occur predominantly through them.

Attenuation of the Wnt Signal Is Required for Stomach Epithelial Differentiation

Mammalian sFRPs function as soluble Wnt antagonists (Finch et al., 1997; Rattner et al., 1997) with a wide spectrum of biochemical and developmental activities. They inhibit Wnt-activated canonical and noncanonical intracellular signaling pathways, and low sFRP concentrations may even potentiate Wnt signals (Uren et al., 2000). To determine if inhibition of Wnt signals could be responsible for gastric epithelial differentiation in mesenchyme-endoderm cocultures, we transfected cells with cDNA encoding Dickkopf (Dkk)1, a secreted Wnt antagonist with mechanisms distinct from those of sFRPs. Whereas sFRPs mimic Frizzled receptors and bind Wnt ligands, Dkk1 interacts with the Wnt coreceptor LRP-5/6 on responding cells, prevents Wnt binding, and selectively antagonizes the canonical pathway (Mao et al., 2001; Semenov et al., 2001). Following treatment with Barx1-specific siRNAs, forced Dkk1 expression in the cultured E12 mesenchyme had the same effect as sFRPs in the mesenchyme-endoderm assay (Figure 6A). Intestine-specific transcripts were reduced significantly, though not always eliminated, whereas expression of all stomach-specific markers was fully restored. The nearly identical activities of Barx1, sFRPs, and Dkk1 in this context strongly implicate a single TF and inhibition of canonical Wnt signal transduction in stomach epithelial specification.

The timing and role of canonical Wnt signaling in stomach development are unknown. To test our prediction that Wnt signals may act especially early in the rostral GI tract, we used TOP-GAL transgenic mice, which express *E. coli LacZ* under the control of a Wnt-responsive promoter that reports faithfully on canonical Wnt signals (DasGupta and Fuchs, 1999). Whereas β-galactosidase activity appears in the intestine only after E15.5, prominent stomach staining is detected as early as E9.5, persists through E12.5, and is attenuated markedly thereafter (Figure 6C). The prolonged stability of β-galactosidase in mammalian cells precludes defining a precise end point, although it is reasonable to infer that the physiologic signal likely is extinguished around E14. The Wnt signal that is transmitted early and transiently in the stomach is entirely confined to the endoderm compartment (Figure 6B), and the timing of Cyclin D1 expression, a known target of Wnt signaling (Tetsu and McCormick, 1999), parallels that of the Wnt activity (Figure 6C). Moreover, the location of Wnt activity, which is prominent over the fundus and body along the greater curvature and is largely excluded from the distal lesser curvature and pylorus, corresponds closely to the distribution of Barx1 expression in the underlying mesenchyme (Figure 6B). Taken together, these data suggest a model wherein a Barx1-induced increase in local sFRP levels limits the extent of canonical Wnt signaling to allow stomach-specific epithelial cell differentiation (Figure 7).

To test this model, we cultured E12.5 stomach endoderm derived from TOP-GAL mouse embryos with wild-type gastric mesenchyme treated with Barx1 siRNA and monitored β-galactosidase activity as a measure of Wnt signaling in the transgenic epithelium. Although interpretation of the results requires consideration of prolonged β-galactosidase stability in mammalian cells, we consistently observed a steep decline in endodermal β-galactosidase activity after the first day of coculture (Figure 6D). Enzyme activity continued to decline, and virtually disappeared, when endoderm was cultured in the presence of control mesenchyme, pointing to attenuation of the Wnt signal as seen in vivo. However, in cultures where mesenchymal Barx1 was reduced by siRNA treatment, canonical Wnt signaling, as reflected in β-galactosidase activity, persisted at significantly higher levels throughout the experiment. Furthermore, the stomach epithelium in Barx1 null mice shows persistent and strong expression of Cyclin D1, a Wnt target whose expression is barely detected in age-matched controls (Figure 6E). The sum of these observations establishes a functional association between mesenchymal Barx1 expression and effects on Wnt signaling in adjacent endoderm.

Discussion

The stomach and intestine diverge from a common primordium to develop distinctive mucosal linings (Karam et al., 1997), muscles, and functions. Differences in gene expression between the two organs prior to epi-

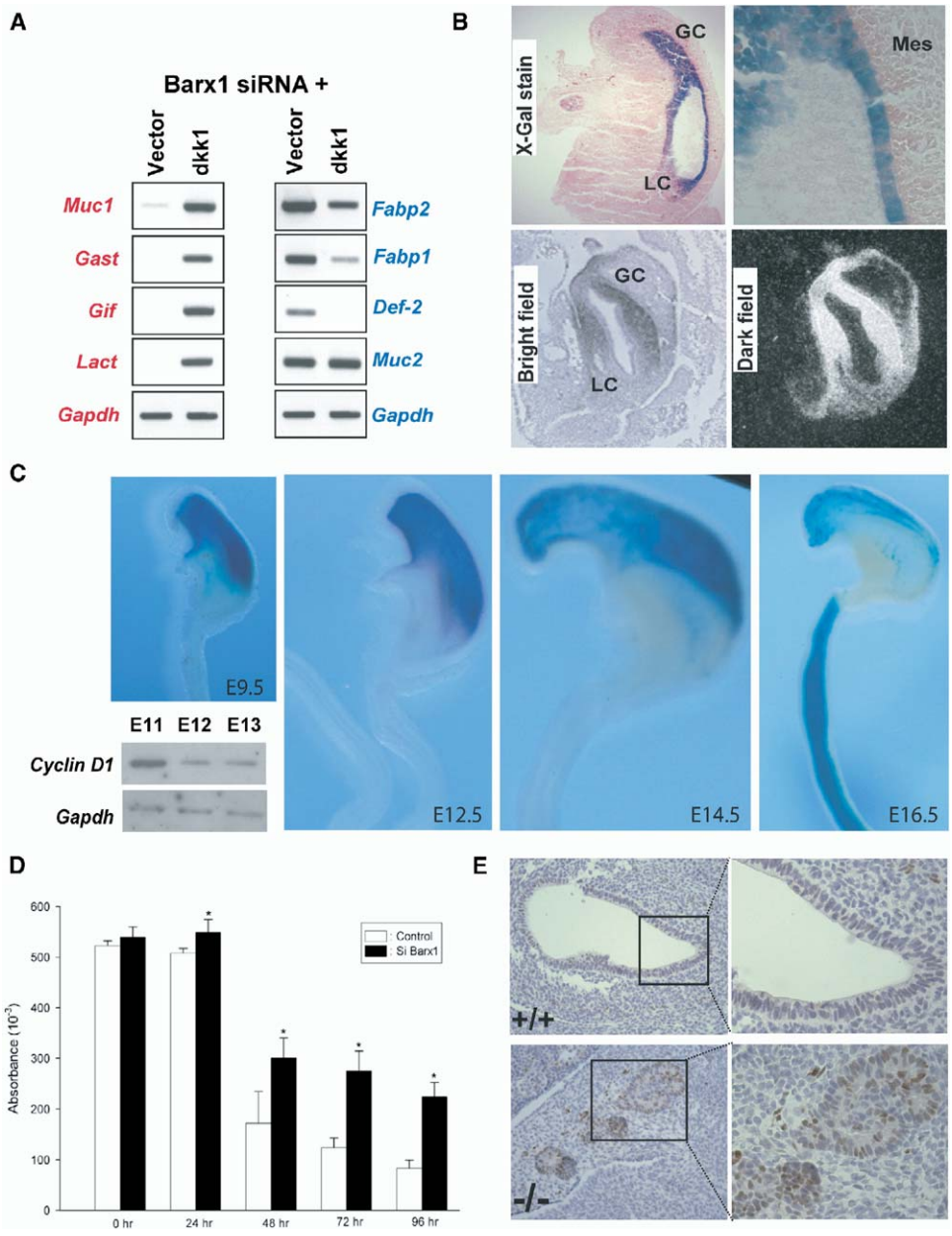

Figure 6. Barx1 Functions to Regulate Wnt Activity in the Prospective Stomach

(A) Rescue of Barx1 siRNA treatment of cultured E12 stomach mesenchyme with forced expression of human Dkk1 cDNA. Recombinant tissue cultures were performed as described earlier, and the results represent two independent experiments.

(B) Anatomic details showing that, in the E12 stomach, Wnt signaling occurs in the endoderm (top panels; left, original magnification 100×; right, magnification 400×) and mostly along the greater curvature (GC); LC, lesser curvature. The lower images show radioactive Barx1 in situ hybridization signals (left, bright field; right, dark field) revealing nearly identical distribution of Barx1 in the stomach wall, concentrated along the greater curvature.

(C) Time course of whole-mount LacZ staining in the stomach and intestine of TOP-GAL mouse embryos at the indicated ages. Cyclin D1 immunoblot (inset) at the indicated ages is consistent with reduced Wnt signaling after E11.

(D) Time course of relative β-galactosidase enzyme activity (y axis) in fetal stomach recombinant cultures of wild-type mesenchyme and TOP-GAL endoderm at the indicated durations after the mesenchyme was treated with either Barx2- (control, white bars) or Barx1-specific (black bars) siRNAs. Results (mean ± SD) are pooled from three independent experiments containing eight samples of each type in aggregate; asterisks indicate a statistically significant increase in enzyme activity with Barx1 siRNA treatment.

(E) Immunohistochemical demonstration of significantly increased Cyclin D1 expression in the E12.5 Barx1$^{-/-}$ epithelium (lower panels) compared to wild-type littermates (top panels).

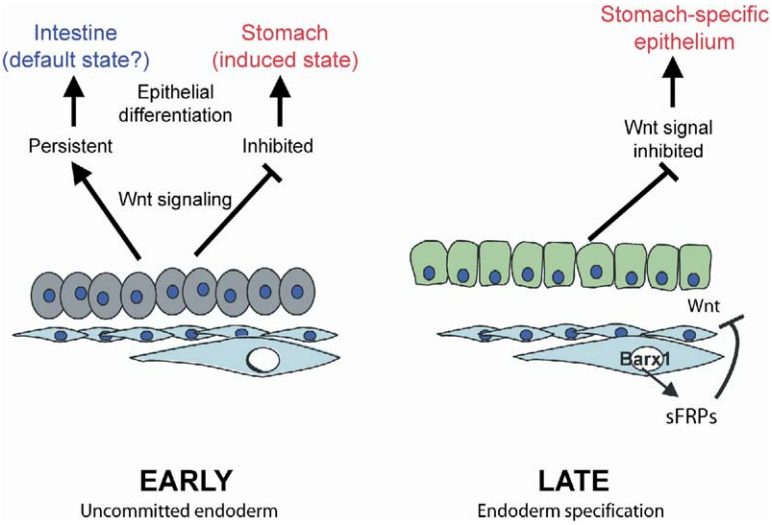

Figure 7. Model for Barx1 Function in Mammalian Stomach Development

Our results indicate that canonical Wnt signaling, which is active in the prospective stomach endoderm early in development, needs to be suppressed to permit stomach epithelial differentiation. In the absence of this suppression, endodermal cells adopt intestinal epithelial character. Antagonism of local Wnt signals in the stomach is achieved through regionally restricted activity of the homeobox TF Barx1, which regulates secretion of sFRPs by stomach mesenchymal cells. This activity directs stomach epithelial differentiation of overlying endoderm.

thelial morphogenesis are informative about the basis for alternative paths in GI differentiation. Barx1 shows the greatest difference of any transcript, and its expression is both tightly controlled and mirrors that of a wave of Wnt signaling in stomach endoderm. To elucidate Barx1 functions, we modified previous experimental models of recombinant fetal cell culture to mimic epithelial development faithfully in molecular terms. The methods rely on separating fetal gut endoderm and mesenchyme and can readily be adapted to investigate other pathways. In embryonic cocultures and knockout mice, Barx1 loss causes the overlying endoderm, normally fated for stomach differentiation, to express an intestine-specific program. These effects are consistent with current models for homeotic transformation of vertebrate visceral organs (Slack, 1985). Barx1 effects are mediated predominantly by secreted Wnt anatagonists, and inhibition of canonical Wnt signaling in the endoderm appears to be a vital element in stomach development. We have thus elucidated a molecular mechanism for the virtual axiom that pattern formation in the developing gut depends on regulated exchange of information between neighboring cells.

Our results point to a transient role for Barx1 during a window in mammalian development when the stomach epithelium is specified (Figure 7), and they highlight the dynamic quality of inductive interactions. Several Wnt proteins and Frizzled receptors appear in fluctuating quantities and patterns throughout vertebrate gut development and in the adult GI tract (McBride et al., 2003; Theodosiou and Tabin, 2003). We show that canonical Wnt signals are transmitted early and abundantly in the prospective stomach, probably to enable some process other than epithelial specification. Barx1 appears transiently in subjacent mesenchyme in much the same distribution, and our observation that sFRP overexpression alone overrides Barx1 deficiency implies that Wnt antagonism is the latter's predominant function. Indeed, Barx1-deficient mesenchyme harbors limited changes in gene expression, some of which likely represent secondary effects, while others may supplant sFRPs in vivo. However, the rostral GI substratum must have a role broader than elaborating sFRPs, because forced Barx1 expression in intestinal mesenchyme has discernible but incomplete effects on endoderm differentiation (Figure 3E). Mesenchymal functions also persist beyond the limited period of Barx1 expression and stomach epithelial specification. In particular, viral misexpression of a cell-autonomous Wnt antagonist in the chick gizzard mesenchyme impairs cytodifferentiation of the overlying epithelium at a stage much later than we investigated in the mouse in this study (Theodosiou and Tabin, 2003). This is one of many examples in which the output of a single signaling pathway depends on the precise context, timing, and localization of signals and target cells.

Our data suggest that intestinal differentiation represents a default state for gut endoderm and that active signals, in the form of Wnt inhibition, are needed to specify the stomach epithelium. Additionally, in our rescue of Barx1 deficiency by either sFRPs or Dkk1, stomach-specific genes were restored more robustly than intestinal gene expression was extinguished, which implies that expression of intestinal genes is especially stable or the preferred outcome in GI development. Perhaps this is why intestinal metaplasia occurs commonly with foregut epithelial injury, whereas the reverse condition, gastric metaplasia of midgut or hindgut derivatives, is rare. Interestingly, forced Wnt signaling in the developing lungs of transgenic mice also induces intestine-type differentiation (Okubo and Hogan, 2004). Thus, intestinal epithelium might represent a common default for all foregut endoderm, requiring Wnt inhibition to permit bronchial or stomach differentiation and other signals to promote pancreatic or hepatic cell fates. In evolutionary terms, the intestine is a primitive structure, whereas both lungs and stomach are recent adaptations; development of a stomach or related foregut-derived digestive organs likely builds on a primitive gut program.

Our observations are hence pertinent to the boundary functions and evolution of homeobox TFs. The developing gut and axial skeleton both rely on clustered Hox genes to establish anatomic domains (Kondo et

al., 1996; Pollock et al., 1992; Roberts et al., 1998; Warot et al., 1997; Wolgemuth et al., 1989). In digestive organs, unclustered homeodomain TFs such as Cdx1, Cdx2, and Pdx1 are expressed throughout life in a restricted distribution, demarcated by sharp anatomic boundaries, and manifest their patterning functions by regulating numerous tissue-specific genes (Beck et al., 2000; Chawengsaksophak et al., 1997; Jonsson et al., 1994; Kim and MacDonald, 2002). In contrast, Barx1 has a transient role, driven by the apparent need for focal antagonism of canonical Wnt signals. The similar distribution of Barx1 (Barlow et al., 1999; Smith et al., 2000) and sFRPs (McBride et al., 2003; Theodosiou and Tabin, 2003) in mouse and chick embryos hints at a developmental pathway shared among land vertebrates. Barx1 is expressed only during organogenesis and is therefore unlikely to participate either in maintaining the stomach mucosa or in preventing intestinal metaplasia in adults. Indeed, diseased metaplastic states differ from the developmental anomaly that occurs in the absence of Barx1. This defect is correctly regarded as heterotopia or transdetermination, because it reflects alternative differentiation of a naïve, uncommitted tissue, whereas metaplasia converts previously specified cells, often long after development is completed. Nevertheless, intestinal metaplasia of the foregut mucosa may result in part from injury-induced reactivation of canonical Wnt signaling in adult life, when Barx1 is not available to inhibit it.

Experimental Procedures

Transcriptional Profiling

Preparation of SAGE libraries was described recently (Lepourcelet et al., 2005); gene annotations were updated in August, 2004. Genes were classified by function according to criteria defined by the Gene Ontology Consortium (http://www.geneontology.org). For oligonucleotide microarray analysis, RNA was prepared 48 hr after siRNA treatment of cultured stomach mesenchyme. Biotinylated cRNA probes were synthesized, fragmented, and hybridized to MOE430A mouse gene chips (Affymetrix). After washing, bound cRNAs were labeled with phycoerythrin-conjugated streptavidin and excited by confocal laser scanning. Three independent Barx1 experiments (two using Barx2 siRNA and one with mock transfection as the control) yielded highly concordant results. Normalization, hybridization image analysis, and comparative expression profiling were performed by using dChip statistical algorithms (Li and Wong, 2001).

Reverse Transcription-PCR

Total cellular RNA was extracted by using Trizol, treated with RNase-free DNase (Ambion), and reverse transcribed with oligo-(dT) primer. First-strand cDNA was used as the template for PCR amplification with AmpliTaq DNA polymerase (Applied Biosystems) for conventional PCR or iQ SYBR Green Supermix (Bio-Rad) for real-time PCR. For conventional PCR, cycle numbers were adjusted to ensure linear amplification; products were resolved by agarose gel electrophoresis and detected by ethidium bromide staining. Real-time PCR was carried out in an iCycler iQ multicolor detection system (Bio-Rad; 94°C for 30 s, 62°C for 30 s, 72°C for 30 s). PCR primers are listed in Table S2. Glyceraldehyde 3-phosphate dehydrogenase (GAPDH) mRNA controlled for equal sample loading.

Northern and Immunoblot Analyses

Total cellular RNA was isolated by using Trizol reagent, separated by formaldehyde-agarose gel electrophoresis, and transferred to a nylon membrane, which was hybridized to α-^{32}P dCTP-labeled 465 bp Barx1 probe and washed to a stringency of 0.1× SSC. Barx1 antisera were produced in rabbits by immunization with His_6-tagged mouse Barx1. Cultured cells were homogenized in lysis buffer (25 mM Tris [pH 7.4], 1 mM EDTA, 0.5% Triton X-100) by sonication. 20 μg protein was resolved over SDS-polyacrylamide 12% gels and transferred to nitrocellulose membranes, which were treated sequentially (1 hr each) with 1% blocking solution (Roche), rabbit Barx1 (1:2000) or GAPDH (1:2000; Abcam) antiserum, and horseradish peroxidase-conjugated goat anti-rabbit IgG (Santa Cruz). Antibody binding was detected by chemiluminescence for 30 s.

In Situ Hybridization and Immunohistochemistry

Radioactive in situ hybridization with ^{35}S-UTP-radiolabeled Barx1 or sFRP2 antisense riboprobes was performed on 8 μm paraffin sections of paraformaldehyde-fixed CD1 or Barx1 mutant mouse embryos, as described (Wilkinson, 1992). Slides were counterstained with hematoxylin (Fluka) and examined by dark-field microscopy. Immunostaining was by the avidin-biotin-peroxidase complex (ABC) method. Paraffin sections (7 μm) were rehydrated and treated successively with warm 0.01 M citrate (pH 6), 40% methanol in 0.3% hydrogen peroxide, and PBS containing 10% goat and 10% fetal bovine sera. Slides were incubated with Cdx2 antibody (BioGenex) diluted in PBS containing 5% goat serum for 24 hr at 4°C in a humid chamber and washed in PBS. After applying biotinylated goat anti-mouse antibody and ABC (Vector Labs), the cytochemical reaction was revealed by staining in diaminobenzidine hydrochloride (Sigma). Images were captured on a CCD camera (QCapture) with Photoshop 7.0 software (Adobe).

Separation and Coculture of Gut Mesenchyme and Endoderm

Organs excised in ice-cold Ca/Mg-free Hank's Balanced Salt Solution (HBSS) were incubated in 10 mM EDTA for 3 min at room temperature and rinsed in HBSS. Endoderm was separated from mesenchyme mechanically by using fine forceps. Mesenchymal cells were treated with 0.03% collagenase (Sigma) for 30 min and with 0.25% trypsin/EDTA (Life Technologies) for 10 min at 37°C, washed in HBSS, and allowed to form monolayers overnight. Fresh endoderm, isolated as above, was cultured over these monolayers 1–3 days later, usually after interim transfection of siRNAs and/or cDNA. Recombinant tissue cultures were done in 6-well dishes, with at least two embryo equivalents of cells per well, leading to nearly confluent layers. Each well contained 2–3 × 10^5 mesenchymal cells and nearly the same number of epithelial cells in Dulbecco's modified Eagle's medium (Life Technologies; supplemented with 2 mM L-glutamine, 100 μg/ml penicillin, 100 U/ml streptomycin, and 20% fetal calf serum) in a humidified incubator at 37°C and 5% CO_2. Cells were harvested at specified times after manipulation, and all experiments were repeated 3–7 times.

siRNA and Gene Overexpression

Barx1 and Barx2 siRNAs were prepared in vitro by using the Silencer siRNA cocktail kit (Ambion), following the manufacturer's recommendations. Briefly, cDNA templates were transcribed in vitro and column-purified dsRNA was digested with 15U RNase III at 37°C for 1 hr. Undigested dsRNA was removed by using a spin-column; resulting siRNA populations were quantified by spectrophotometry and visualized on nondenaturing 20% polyacrylamide gels. Constructs to overexpress murine Barx1 and sFRPs were generated in pIRES2-EGFP (Clontech). Flag epitope-tagged human Dkk1 plasmid (Semenov et al., 2001) was provided by Xi He (Children's Hospital, Boston, MA). siRNAs were transfected by using siPORT *Lipid* and siPORT *Amine* agents (Ambion), and plasmids were introduced the following day by using Transfectin (Bio-Rad).

Mouse Strains

We generated BarX1 knockout mice on an inbred 129/Sv background, by using standard targeting methods in mouse embryonic stem cells; details will be reported separately. TOP-GAL reporter mice were purchased from Jackson Laboratories and maintained on the BALB/c background. Animals were housed and handled according to protocols approved by institutional committees.

β-Galactosidase Detection

Following fixation with 4% paraformaldehyde, whole embryos or isolated organs were washed three times in phosphate-buffered saline (PBS) and incubated in staining solution (PBS, 1 mg/ml 5-bromo-4-chloro-3-indoyl-β-D-galactoside [Invitrogen], 5 mM $K_3Fe(CN)_6$, 5 mM $K_4Fe(CN)_6 \cdot 3H_2O$, 1 mM $MgCl_2$, 0.01% sodium desoxycholate, 0.02% NP-40) for 9–10 hr at 37°C. After whole-mount photography, samples were postfixed in 4% paraformaldehyde for 1 hr at 4°C, dehydrated, embedded in paraffin, sectioned, and examined under a compound microscope. To measure enzyme activity in cultured tissue explants, we used the Enhanced β-Galactosidase Assay Kit (Gene Therapy Systems) according to the manufacturer's protocol. Recombinant enzyme was used to generate a standard curve, and differences between eight samples with each treatment (pooled from three independent experiments) were evaluated by the Student's t test.

Supplemental Data

Supplemental Data including tables listing significant differences in gene expression between E12 mouse intestine and stomach and oligonucleotide primers used for RT-PCR analysis are available at http://www.developmentalcell.com/cgi/content/full/8/4/611/DC1/.

Acknowledgments

This work was supported by the Robert Black Charitable Foundation, the National Institutes of Health (R01-DK61139), the Wellcome Trust, and the United Kingdom Medical Research Council. R.A.S. is a Scholar of the Leukemia and Lymphoma Society. We thank K. Kinzler for permission to use SAGE; L. Cai and M. Hu for computer analyses; M. Bradman, M. Lepourcelet, Q. Liu, and E. Shin for technical assistance; J. Goodwin, C. Healy, and S. Pachecofor for help with Barx1$^{-/-}$ mice; M. Semenov and X. He for Dkk1 plasmid; S. Parkinson and M. Loda for helpful discussions; and M. Choi, J. Green, and S.H. Orkin for critical manuscript review. The authors declare no financial conflicts of interest.

Received: January 10, 2005
Revised: January 10, 2005
Accepted: January 18, 2005
Published: April 4, 2005

References

Aubin, J., Dery, U., Lemieux, M., Chailler, P., and Jeannotte, L. (2002). Stomach regional specification requires Hoxa5-driven mesenchymal-epithelial signaling. Development *129*, 4075–4087.

Barlow, A.J., Bogardi, J.P., Ladher, R., and Francis-West, P.H. (1999). Expression of chick Barx-1 and its differential regulation by FGF-8 and BMP signaling in the maxillary primordia. Dev. Dyn. *214*, 291–302.

Beck, F., Tata, F., and Chawengsaksophak, K. (2000). Homeobox genes and gut development. Bioessays *22*, 431–441.

Chawengsaksophak, K., James, R., Hammond, V.E., Kontgen, F., and Beck, F. (1997). Homeosis and intestinal tumours in Cdx2 mutant mice. Nature *386*, 84–87.

Cheng, H., and Leblond, C.P. (1974). Origin, differentiation and renewal of the four main epithelial cell types in the mouse small intestine. V. Unitarian theory of the origin of the four epithelial cell types. Am. J. Anat. *141*, 537–561.

DasGupta, R., and Fuchs, E. (1999). Multiple roles for activated LEF/TCF transcription complexes during hair follicle development and differentiation. Development *126*, 4557–4568.

Duluc, I., Freund, J.N., Leberquier, C., and Kedinger, M. (1994). Fetal endoderm primarily holds the temporal and positional information required for mammalian intestinal development. J. Cell Biol. *126*, 211–221.

Finch, P.W., He, X., Kelley, M.J., Uren, A., Schaudies, R.P., Popescu, N.C., Rudikoff, S., Aaronson, S.A., Varmus, H.E., and Rubin, J.S. (1997). Purification and molecular cloning of a secreted, Frizzled-related antagonist of Wnt action. Proc. Natl. Acad. Sci. USA *94*, 6770–6775.

Hayashi, K., Yasugi, S., and Mizuno, T. (1988). Pepsinogen gene transcription induced in heterologous epithelial-mesenchymal recombinations of chicken endoderms and glandular stomach mesenchyme. Development *103*, 725–731.

Hebrok, M., Kim, S.K., and Melton, D.A. (1998). Notochord repression of endodermal Sonic hedgehog permits pancreas development. Genes Dev. *12*, 1705–1713.

Jonsson, J., Carlsson, L., Edlund, T., and Edlund, H. (1994). Insulin-promoter-factor 1 is required for pancreas development in mice. Nature *371*, 606–609.

Jung, J., Zheng, M., Goldfarb, M., and Zaret, K.S. (1999). Initiation of mammalian liver development from endoderm by fibroblast growth factors. Science *284*, 1998–2003.

Kaestner, K.H., Silberg, D.G., Traber, P.G., and Schutz, G. (1997). The mesenchymal winged helix transcription factor Fkh6 is required for the control of gastrointestinal proliferation and differentiation. Genes Dev. *11*, 1583–1595.

Karam, S.M., Li, Q., and Gordon, J.I. (1997). Gastric epithelial morphogenesis in normal and transgenic mice. Am. J. Physiol. *272*, G1209–G1220.

Kedinger, M., Simon-Assmann, P.M., Lacroix, B., Marxer, A., Hauri, H.P., and Haffen, K. (1986). Fetal gut mesenchyme induces differentiation of cultured intestinal endodermal and crypt cells. Dev. Biol. *113*, 474–483.

Kim, S.K., and MacDonald, R.J. (2002). Signaling and transcriptional control of pancreatic organogenesis. Curr. Opin. Genet. Dev. *12*, 540–547.

Kondo, T., Dolle, P., Zakany, J., and Duboule, D. (1996). Function of posterior HoxD genes in the morphogenesis of the anal sphincter. Development *122*, 2651–2659.

Lepourcelet, M., Tou, L., Cai, L., Sawada, J., Lazar, A.J.F., Glickman, J.N., Williamson, J.A., Everett, A.D., Redston, M., Fox, E.A., et al. (2005). Insights into developmental mechanisms and cancers in the mammalian intestine derived from SAGE and study of the hepatoma-derived growth factor (HDGF). Development *132*, 415–427.

Li, C., and Wong, W.H. (2001). Model-based analysis of oligonucleotide arrays: expression index computation and outlier detection. Proc. Natl. Acad. Sci. USA *98*, 31–36.

Mao, B., Wu, W., Li, Y., Hoppe, D., Stannek, P., Glinka, A., and Niehrs, C. (2001). LDL-receptor-related protein 6 is a receptor for Dickkopf proteins. Nature *411*, 321–325.

McBride, H.J., Fatke, B., and Fraser, S.E. (2003). Wnt signaling components in the chicken intestinal tract. Dev. Biol. *256*, 18–33.

Mizuno, T., and Yasugi, S. (1990). Susceptibility of epithelia to directive influences of mesenchymes during organogenesis: uncoupling of morphogenesis and cytodifferentiation. Cell Differ. Dev. *31*, 151–159.

Okubo, T., and Hogan, B.L. (2004). Hyperactive Wnt signaling changes the developmental potential of embryonic lung endoderm. J. Biol. *3*, 11.11–11.17.

Perreault, N., Katz, J.P., Sackett, S.D., and Kaestner, K.H. (2001). Foxl1 controls the Wnt/beta-catenin pathway by modulating the expression of proteoglycans in the gut. J. Biol. Chem. *276*, 43328–43333.

Pollock, R.A., Jay, G., and Bieberich, C.J. (1992). Altering the boundaries of Hox3.1 expression: evidence for antipodal gene regulation. Cell *71*, 911–923.

Ramalho-Santos, M., Melton, D.A., and McMahon, A.P. (2000). Hedgehog signals regulate multiple aspects of gastrointestinal development. Development *127*, 2763–2772.

Rattner, A., Hsieh, J.C., Smallwood, P.M., Gilbert, D.J., Copeland, N.G., Jenkins, N.A., and Nathans, J. (1997). A family of secreted proteins contains homology to the cysteine-rich ligand-binding domain of frizzled receptors. Proc. Natl. Acad. Sci. USA *94*, 2859–2863.

Reid, B.J., Levine, D.S., Longton, G., Blount, P.L., and Rabinovitch,

P.S. (2000). Predictors of progression to cancer in Barrett's esophagus: baseline histology and flow cytometry identify low- and high-risk patient subsets. Am. J. Gastroenterol. *95*, 1669–1676.

Roberts, D.J., Johnson, R.L., Burke, A.C., Nelson, C.E., Morgan, B.A., and Tabin, C. (1995). Sonic hedgehog is an endodermal signal inducing Bmp-4 and Hox genes during induction and regionalization of the chick hindgut. Development *121*, 3163–3174.

Roberts, D.J., Smith, D.M., Goff, D.J., and Tabin, C.J. (1998). Epithelial-mesenchymal signaling during the regionalization of the chick gut. Development *125*, 2791–2801.

Rossi, J.M., Dunn, N.R., Hogan, B.L., and Zaret, K.S. (2001). Distinct mesodermal signals, including BMPs from the septum transversum mesenchyme, are required in combination for hepatogenesis from the endoderm. Genes Dev. *15*, 1998–2009.

Semenov, M.V., Tamai, K., Brott, B.K., Kuhl, M., Sokol, S., and He, X. (2001). Head inducer Dickkopf-1 is a ligand for Wnt coreceptor LRP6. Curr. Biol. *11*, 951–961.

Silberg, D.G., Swain, G.P., Suh, E.R., and Traber, P.G. (2000). Cdx1 and cdx2 expression during intestinal development. Gastroenterology *119*, 961–971.

Silberg, D.G., Sullivan, J., Kang, E., Swain, G.P., Moffett, J., Sund, N.J., Sackett, S.D., and Kaestner, K.H. (2002). Cdx2 ectopic expression induces gastric intestinal metaplasia in transgenic mice. Gastroenterology *122*, 689–696.

Slack, J.M.W. (1985). Homoeotic transformations in man: implications for the mechanism of embryonic development and for the organization of epithelia. J. Theor. Biol. *114*, 463–490.

Smith, D.M., Grasty, R.C., Theodosiou, N.A., Tabin, C.J., and Nascone-Yoder, N.M. (2000). Evolutionary relationships between the amphibian, avian, and mammalian stomachs. Evol. Dev. *2*, 348–359.

Stappenbeck, T.S., Wong, M.H., Saam, J.R., Mysorekar, I.U., and Gordon, J.I. (1998). Notes from some crypt watchers: regulation of renewal in the mouse intestinal epithelium. Curr. Opin. Cell Biol. *10*, 702–709.

Sukegawa, A., Narita, T., Kameda, T., Saitoh, K., Nohno, T., Iba, H., Yasugi, S., and Fukuda, K. (2000). The concentric structure of the developing gut is regulated by Sonic hedgehog derived from endodermal epithelium. Development *127*, 1971–1980.

Tetsu, O., and McCormick, F. (1999). Beta-catenin regulates expression of cyclin D1 in colon carcinoma cells. Nature *398*, 422–426.

Theodosiou, N.A., and Tabin, C.J. (2003). Wnt signaling during development of the gastrointestinal tract. Dev. Biol. *259*, 258–271.

Tissier-Seta, J.P., Mucchielli, M.L., Mark, M., Mattei, M.G., Goridis, C., and Brunet, J.F. (1995). Barx1, a new mouse homeodomain transcription factor expressed in cranio-facial ectomesenchyme and the stomach. Mech. Dev. *51*, 3–15.

Tucker, A., and Sharpe, P. (2004). The cutting-edge of mammalian development; how the embryo makes teeth. Nat. Rev. Genet. *5*, 499–508.

Uren, A., Reichsman, F., Anest, V., Taylor, W.G., Muraiso, K., Bottaro, D.P., Cumberledge, S., and Rubin, J.S. (2000). Secreted frizzled-related protein-1 binds directly to Wingless and is a biphasic modulator of Wnt signaling. J. Biol. Chem. *275*, 4374–4382.

van de Wetering, M., Sancho, E., Verweij, C., de Lau, W., Oving, I., Hurlstone, A., van der Horn, K., Batlle, E., Coudreuse, D., Haramis, A.P., et al. (2002). The beta-catenin/TCF-4 complex imposes a crypt progenitor phenotype on colorectal cancer cells. Cell *111*, 241–250.

van den Brink, G.R., Hardwick, J.C., Tytgat, G.N., Brink, M.A., Ten Kate, F.J., Van Deventer, S.J., and Peppelenbosch, M.P. (2001). Sonic hedgehog regulates gastric gland morphogenesis in man and mouse. Gastroenterology *121*, 317–328.

Velculescu, V.E., Zhang, L., Vogelstein, B., and Kinzler, K.W. (1995). Serial analysis of gene expression. Science *270*, 484–487.

Warburton, D., Schwarz, M., Tefft, D., Flores-Delgado, G., Anderson, K.D., and Cardoso, W.V. (2000). The molecular basis of lung morphogenesis. Mech. Dev. *92*, 55–81.

Warot, X., Fromental-Ramain, C., Fraulob, V., Chambon, P., and Dolle, P. (1997). Gene dosage-dependent effects of the Hoxa-13 and Hoxd-13 mutations on morphogenesis of the terminal parts of the digestive and urogenital tracts. Development *124*, 4781–4791.

Wells, J.M., and Melton, D.A. (1999). Vertebrate endoderm development. Annu. Rev. Cell Dev. Biol. *15*, 393–410.

Wilkinson, D.G. (1992). In Situ Hybridization: A Practical Approach (Oxford, UK: IRL Press).

Wolgemuth, D.J., Behringer, R.R., Mostoller, M.P., Brinster, R.L., and Palmiter, R.D. (1989). Transgenic mice overexpressing the mouse homoeobox-containing gene Hox-1.4 exhibit abnormal gut development. Nature *337*, 464–467.

Yokouchi, Y., Sakiyama, J., and Kuroiwa, A. (1995). Coordinated expression of Abd-B subfamily genes of the HoxA cluster in the developing digestive tract of chick embryo. Dev. Biol. *169*, 76–89.

Zhang, J., Rosenthal, A., de Sauvage, F.J., and Shivdasani, R.A. (2000). Downregulation of hedgehog signaling is required for organogenesis of the small intestine in *Xenopus*. Dev. Biol. *229*, 188–202.